ACS APPLIED NANO MATERIALS

Thermodynamic−Kinetic Synergistic Separation for O_2/N_2 and CO_2/CH_4 on Nanoporous Carbon Molecular Sieves

Liangjun Li,* Dandan Liu, Dewen Zhen,* Zhixing Ge, Xi Zhang, Bo Xiong, Zhi Li, Kuitong Zhang, Tao Xing, Wenli Xu, Fuzhao Zhang, Xin Gu, Pengcheng Dai, and Xuebo Zhao*

Cite This: *ACS Appl. Nano Mater.* 2022, 5, 11414−11422

Read Online

ACCESS | Metrics & More | Article Recommendations | Supporting Information

Downloaded via CHINA UNIV OF PETROLEUM on October 11, 2022 at 02:31:43 (UTC).
See https://pubs.acs.org/sharingguidelines for options on how to legitimately share published articles.

ABSTRACT: Carbon molecular sieves (CMSs) are the key adsorbents for gas separation through pressure swing adsorption (PSA), a promising technique that has found many applications in air separation and natural gas purification. However, the current process of preparing CMSs with finely tuned nanopores based on the repeated CVD process is technically challenging and energy-consuming. In this work, we report a facial method of preparing CMSs through the one-step carbonization of a metal−organic framework. The direct carbonization of an *rht*-type metal−organic framework (MOF) affords a type of CMSs with an ultramicro−nanoporous structure that is comparable with the kinetic diameter of small gases (N_2, O_2, CO_2, and CH_4). As a result, this type of CMSs shows significant differences in both equilibrium adsorption properties and diffusion rates for O_2/N_2 and CO_2/CH_4. The kinetic separation coefficient for O_2/N_2 and CO_2/CH_4 is high up to 47 and 105, respectively. In addition to excellent equilibrium and kinetic selectivity, this MOF-CMS shows compatibility between equilibrium and kinetic adsorption properties, giving rise to a thermodynamic−kinetic synergistic effect for O_2/N_2 and CO_2/CH_4 separation. These outstanding separation performances can be attributed to the ultramicro−nanopores of CMSs, which are modulated by the uniform pore structure of the MOF precursor. The high selectivity combined with the facial preparation process for this CMS may open an avenue of preparing nanoporous CMSs with desired functionalities.

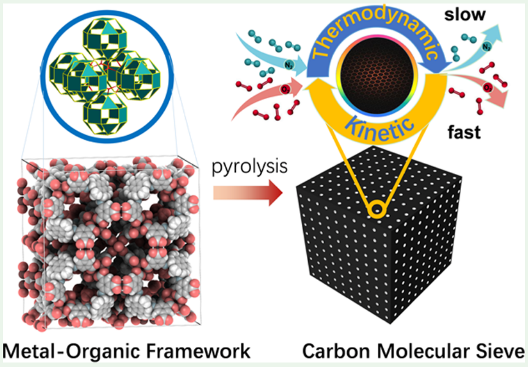

KEYWORDS: *carbon molecular sieve, metal−organic frameworks, gas separation, adsorption kinetics, thermodynamic−kinetic synergistic adsorption*

■ INTRODUCTION

Pressure swing adsorption (PSA) is a promising technique of gas separation alternative to the conventional cryogenic process.[1−3] The advantages including high energy efficiency, low plant investment, and easy mobility endow this technique with promising potentials for a wide range of applications, especially for those plants with different scales or high mobility.[4,5] Generally, gas separation through the PSA technique can be achieved based on either equilibrium or kinetic mechanisms.[6] PSA-based air purification is a typical process based on the kinetic separation mechanism in which the difference in kinetic rates is the driving force.[7,8] In this process, the efficient discrimination of O_2 and N_2 molecules through different diffusion rates raises a high requirement for the pores of the adsorbent, given that O_2 and N_2 molecules exhibit high similarity in both physical properties and kinetic diameters.[7] In contrast to O_2/N_2 separation, the PSA-based CO_2/CH_4 separation is a typical thermodynamic process that is driven by the different thermodynamic adsorption properties of CO_2 and CH_4 molecules on adsorbents.[9] To improve the CO_2/CH_4 separation selectivity, several strategies, such as increasing anchoring Lewis basic sites,[10] optimizing pore structures,[11,12] etc., have been utilized to increase the interaction strength of CO_2 molecules with adsorbents, whereas the increasing interaction strength also leads to higher regeneration energy and higher cost required in the regeneration process of adsorbents in industrial applications. In fact, the conflict between selectivity and regeneration cost has raised a limitation to the applicability of highly affinitive adsorbents in practical applications.[13]

Compared to the gas separation process driven by single thermodynamic or kinetic differences, a separation driven by dual forces, namely the thermodynamic−kinetic synergistic separation, could largely improve the gas separation efficiency if the kinetic rate sequence of gas components is compatible with their thermodynamic adsorption properties (e.g., higher equilibrium CO_2 uptakes corresponding to faster CO_2

Received: June 6, 2022
Accepted: July 29, 2022
Published: August 11, 2022

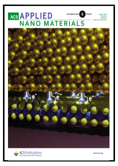

ACS Publications © 2022 American Chemical Society

https://doi.org/10.1021/acsanm.2c02469

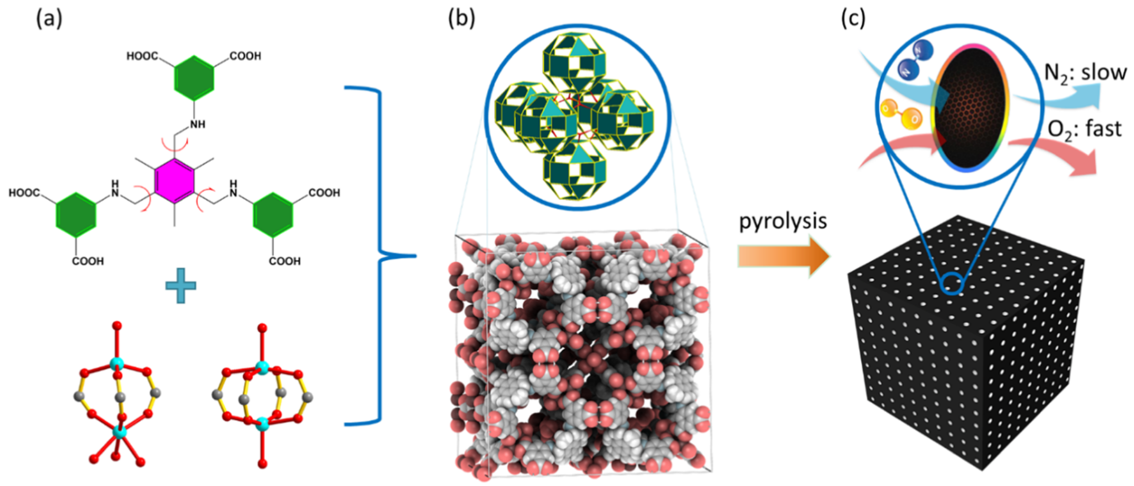

Figure 1. Schematic illustration of the preparation of MOF-CMS. (a) Ligand for the MOF precursor: H_6L and $[Zn_2(COO)_3(H_2O)_4]$ and $[Zn_2(COO)_4(H_2O)_2]$ SBUs; (b) packing mode presentation of the crystallographic structure for the MOF precursor and its simplified network; and (c) illustration of the CMS derived from the pyrolysis of the MOF.

diffusion rates). In recent years, such thermodynamic−kinetic synergistic separation has been regarded as an emerging strategy to enhance the gas separation efficiency.[14,15] However, to realize such a process, fabricating functional adsorbents with a significant difference in the thermodynamic properties and compatible kinetic rate sequence for CO_2/CH_4 molecules is the prerequisite, and the efficient preparation process of such adsorbents has rarely been reported to date.[16,17]

Carbon molecular sieves (CMSs), which exhibit finely tailored nanopores, are the key adsorbents in the PSA process.[18,19] For CMSs, the nanoscale porous structure is the key structural parameter that determines the separation efficiency for gas mixtures. Given the high similarity in the kinetic diameters for O_2, N_2, CO_2, and CH_4 molecules (O_2: 0.346 nm; N_2: 0.364 nm; CO_2: 0.33 nm CH_4: 0.382 nm), the efficient separation for O_2/N_2 and CO_2/CH_4 gas mixtures requires finely tailored nanoporous structures. Currently, the process of preparing CMSs is based on the chemical vapor deposition (CVD) combined with physical/chemical activation technique, which is always fuzzy and empirical.[20,21] To tune the nanopores of CMSs to a certain range, a complicated multistep repetitive CVD and physical/chemical activation process is always required in the industrial production process. Although the nanopore aperture of the resultant CMS can be regulated artificially through such a process, it leads to a high cost of the resulting CMS products.[20,22] Furthermore, this complicated process could also give rise to the uneven quality of the resulting CMS product, thus decreasing the production rate.

In recent years, metal−organic frameworks (MOFs) represent an emerging family of crystalline materials with uniform structures, amenable pore environments, and tunable functionalities.[23,24] In addition to their promising potentials in a large field of applications, they are also ideal precursors or templates for constructing functional carbons, which have attracted extensive research interests in recent years. Owing to the great flexibility in tuning pore structures and functionalities in MOF precursors, several types of MOF-derived carbons with special functionalities have been synthesized based on the bottom-up strategy, and their performance in gas storage,[25] CO_2 separation,[26] catalysis,[27] energy storage,[28] etc. have been intensively investigated. In this work, we propose a new strategy of preparing CMSs through one-step carbonization of MOFs. The structural study reveals that this type of CMS possesses uniform pore diameters, which are comparable with the kinetic diameters of small gas molecules. The adsorption studies demonstrate that this CMS not only exhibits excellent thermodynamic adsorption selectivities for O_2/N_2 and CO_2/CH_4 but also shows outstanding kinetic differences for O_2/N_2 and CO_2/CH_4. The faster diffusion rates of CO_2 and O_2 are compatible with their preferable adsorption on adsorbents, which gives rise to an outstanding separation performance under a thermodynamic−kinetic synergistic adsorption separation mechanism. These results not only disclose a facile method of preparing CMSs but also provide a strategy for fabricating adsorbents with a thermodynamic−kinetic synergistic adsorption separation effect, which could also pave a new way of preparing CMSs with new structures and new functionalities.

■ RESULTS AND DISCUSSION

This CMS is derived from one-step carbonization of a flexible MOF, $[Zn_3L(H_2O)_3]$ (L = 5,5′-(1,3,5-trimethyl-2,4,6-phenylene)-tri(methylene)-tri(azanediyl) tri-isophthalate acid, H_6L) (see the preparation procedures in Figure 1). The ligand H_6L is synthesized from the substitution reaction of 5-amino-isophthalic acid dimethyl ester and 2,4,6-tris(bromomethyl)-mesitylene, followed by the ester hydrolysis and acidification reaction. The solvothermal reaction between H_6L and $Zn(NO_3)_2{\cdot}6(H_2O)$ at 80 °C in a mixed solution of DMF/EtOH/Water (3/3/2) for 48 h gives rise to large and colorless polyhedral single crystals (see the experimental details in the Supporting Information, S1).

Single-crystal X-ray diffraction analysis reveals a three-dimensional network, which is new in the MOF family. Crystallographic data demonstrate that this MOF crystallizes in a high symmetrical *cubic* system, with the space group $Fm\bar{3}m$ (see the crystal parameters in Table S1 in the Supporting Information). The coordination of the Zn^{2+} ions with the carboxylate groups gives rise to two types of paddle-wheel secondary building units (SBUs): the 3-connected triangular $[Zn_2(COO)_3(H_2O)_4]$ and the 4-connected square $[Zn_2(COO)_4(H_2O)_2]$ (see Figure 1a). These two types of SBUs are further linked by isophthalate groups to afford a

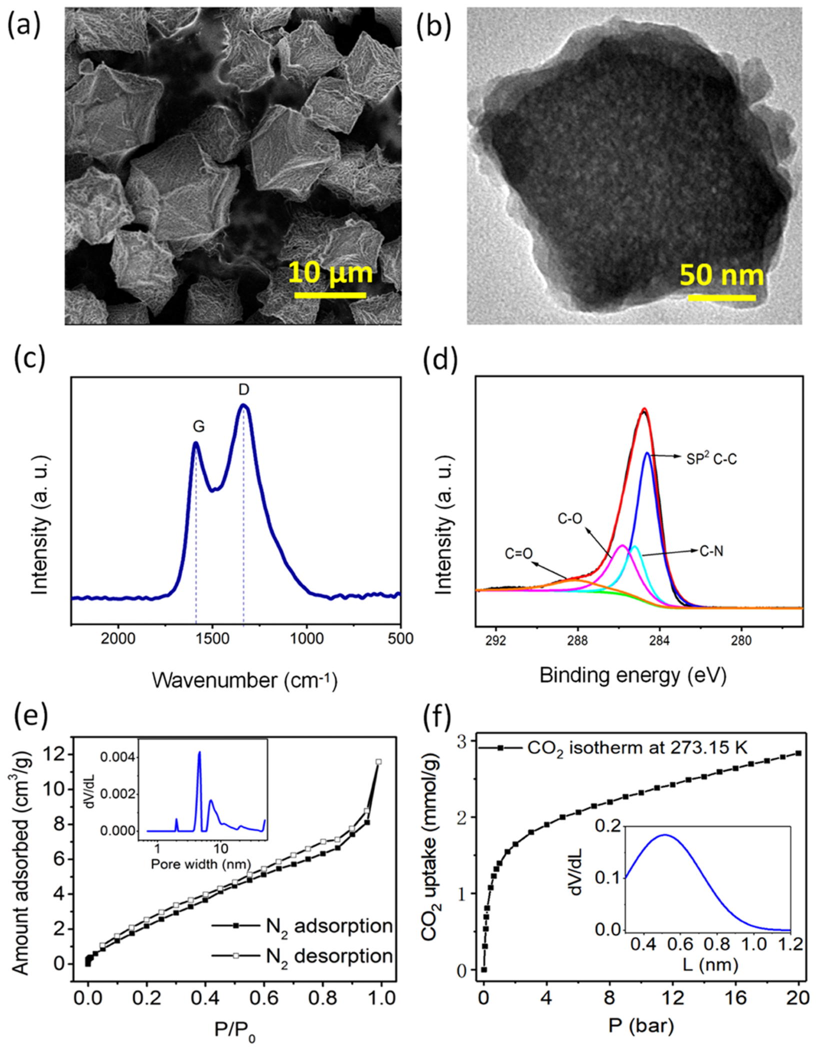

Figure 2. (a) SEM photograph of MOF-CMS; (b) TEM photograph of MOF-CMS; (c) Raman spectra for MOF-CMS; (d) C 1s XPS spectra for MOF-CMS; (e) N_2 isotherm at 77 K on the MOF-CMS (insertion: pore size distribution of the MOF-CMS derived from the NLDFT method on the basis of the N_2 isotherm); and (f) CO_2 isotherm at 273.15 K on MOF-CMS (insertion: pore size distribution calculated from DRS analysis based on the CO_2 isotherm).

cuboctahedron-shaped cage with 24 nodes.[29] Due to the steric hindrance of three methyl groups decorated on the central phenyl ring, the side isophthalate groups twist to a plane perpendicular to the central phenyl ring. Caused by the twist, the ligand exhibits a special steric configuration with a D_{3h} symmetry. Noteworthily, such a configuration is different from conventional planar ligands which adopt a simple C_3 symmetry. As a result, a (3–24)-connected *rht* net is formed by linking the 6-connected D_{3h} ligand with 3- and 4-connected SBUs (as shown in Figure 1b). With simplifying $[Zn_2(COO)_3(H_2O)_4]$, $[Zn_2(COO)_4(H_2O)_2]$, and H_6L into 3-, 4-, and 6-connected nodes, respectively, the framework of this MOF can be simplified into a (3,4,6)-connected framework. Notably, this topology is a variant of the usual *rht* net formed by C_3-symmertric ligands and 4-connected paddle-wheel SBUs[30] and is a rare topology that is only reported once in our previous study.[29] Owing to the combined effect of the *rht* network and large size H_6L ligand, this MOF exhibits rather high porosity, achieving a high porosity ratio of 71.6%. Large cages with diameters of up to 2 nm and windows (0.7 nm) are involved in this MOF. The theoretical surface area for this MOF calculated from single-crystal data reaches 3433 m^2/g, with a pore volume of 1.124 cm^3/g. However, due to the high porosity and flexibility of the ligand, this MOF does not show permanent porosity after activation, although many activation methods have been tried. The negligible BET surface area after activation suggests that the porosity is collapsed due to its fragile framework.

In spite of this, the large crystals of this MOF can be transferred into a CMS when subjected to a thermal treatment process (termed MOF-CMS; see the experimental details in the Supporting Information, S1). The TGA profile shows that the MOF is completely decomposed above 550 °C under a N_2 atmosphere (see the TGA profile in Figure S3 in the Supporting Information). After one-step carbonization of the MOF precursor at 600 °C under a N_2 atmosphere, a type of dense solid with polyhedron morphology can be obtained (as shown in the SEM pictures in Figure 2a). With carbonization, the fragile MOF transforms into stable carbon materials. The as-prepared MOF-CMS inherits the polyhedron morphology of the MOF crystals. The grain size is about 100 μm, which is only about 1/3 of the size of MOF precursors. This phenomenon suggests that the MOF crystals undergo a substantial shrinkage upon pyrolysis. TEM images reveal a

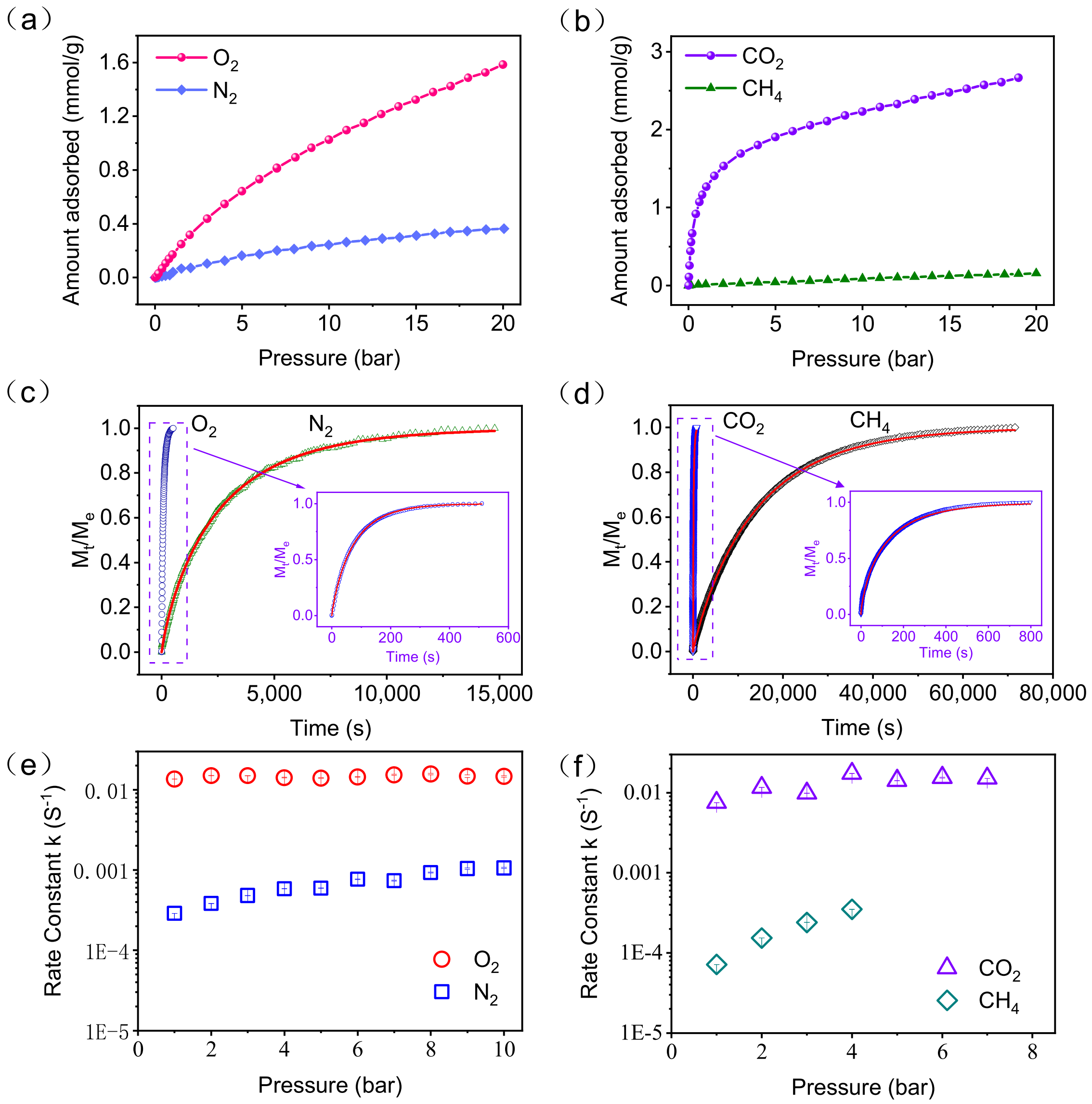

Figure 3. (a) Adsorption isotherms of N_2 and O_2 at 293.15 K on the MOF-CMS; (b) adsorption isotherms of CH_4 and CO_2 at 293.15 K on the MOF-CMS; (c) kinetic profiles for N_2 and O_2 adsorption on the MOF-CMS in the pressure range of 1000−1500 mbar at 293.15 K (the red curve represents the simulated kinetic profile for N_2 and O_2 (inset)); (d) kinetic profiles for CO_2 and CH_4 adsorption on the MOF-CMS in the pressure range of 1000−1500 mbar at 293.15 K (the red curve represents the simulated kinetic profile for CH_4 and CO_2 (inset)); (e) variation of the stretched exponential rate constants of O_2 and N_2 with different pressures at 293 K; and (f) variation of the stretched exponential rate constants of CO_2 and CH_4 with different pressures at 293 K.

characteristic of amorphous carbon, with some mesopores in the internal space of the carbon. Two broad peaks around 24 and 44° in the PXRD pattern can be assigned to the characteristic peaks of amorphous carbon (see the PXRD patterns in the Supporting Information, S3). Raman spectroscopy displays an I_D/I_G value of 1.2, suggesting that it possesses a rather high content of sp^3 carbon (as shown in Figure 2c). X-ray photoelectron spectroscopy (XPS) for C reveals that sp^2-type C, C-O, C═O, and C-N groups are involved in the carbon matrix (as shown in Figure 2d).

The N_2 isotherm at 77 K on the MOF-CMS exhibits a type-II isotherm according to the IUPAC scheme (as shown in Figure 2e). It exhibits a BET surface area of 11.9 m^2/g and a pore volume of 0.0179 cm^3/g, behaving like a nonporous carbon. The pore size distribution calculated from nonlocal density functional theory (NLDFT) based on the N_2 isotherm at 77 K shows a hierarchical pore structure centered at 1.7 and 4.0 nm. To get a more comprehensive understanding of the pore structure, the pore structure of the MOF-CMS is also evaluated using CO_2 as the probe molecule. It has been reported that CO_2 is a more suitable reference gas for pore structural characterization with ultramicropores due to the diffusional issues of N_2 molecules at cryogenic temperature.[31−33] Based on the CO_2 isotherm at 273.15 K, the Dubinin−Radushkevich−Stoeckl (DRS) analysis shows a pore size distribution centered at 0.46 nm, which belongs to ultramicropores, as shown in Figure 2f. The pore diameter is smaller than that of the commercial 1.5-GN-H CMS used for air separation.[18]

The isotherms of N_2, O_2, CO_2, and CH_4 at ambient temperatures were measured on the MOF-CMS to investigate its thermodynamic gas sorption properties. As shown in Figure 3a, the MOF-CMS shows an O_2 uptake of 0.17 mmol/g at 1 bar and 293 K, while the N_2 uptake is only about 0.04 mmol/g under the same conditions. Therefore, from the view of thermodynamics, O_2 is preferentially adsorbed on the CMS compared to N_2. This phenomenon is contrary to that of common adsorbents such as porous carbon or zeolite in which N_2 is always preferentially adsorbed.[34,35] However, the higher uptake of O_2 over N_2 is agreeable with the results of some CMSs. The adsorption selectivity in favor of O_2 could be attributed to the kinetic-controlled diffusion due to the comparable kinetic diameters of gas molecules and pore dimensions. It has been reported that the pores with a diameter very similar to molecular kinetic diameters could lead to an active adsorption due to the overlap of potential adsorption profiles with the creation of a stronger adsorption field.[36] Furthermore, the possible formation of dimers in the micropores for N_2 molecules could also induce restrictions of N_2 diffusion into the ultramicropores of CMS, leading to its lower uptakes and slower diffusion rates than O_2.

Based on adsorption isotherms, the equilibrium adsorption selectivity for the O_2/N_2 mixture can be evaluated by ideal adsorbed solution theory (IAST), which has been widely validated by several studies.[4,37] At the feed gas ratio of 50/50 and the pressure of 1 bar, the IAST selectivity for the O_2/N_2 mixture is calculated as 6.08 (see the calculation procedures in the Supporting Information, S5). This value is among the high ranks in adsorbents and is significantly higher than that of common porous carbon.[38] The high adsorption selectivity of O_2/N_2 could be attributed to the discrimination effects on N_2 molecules induced by the ultramicropores of the MOF-CMS. The high adsorption potential of ultramicropores in the MOF-CMS can also enhance the adsorption selectivity of O_2 molecules.

As shown in Figure 3b, the MOF-CMS exhibits distinct isotherms for CO_2 and CH_4. The adsorption uptake of CO_2 increases rapidly at the low-pressure range and gradually reaches saturation at the higher pressure range owing to the small pore volume of the MOF-CMS. The CO_2 uptake of 1.26 mmol/g at 293.15 K and 1 bar is 31.7 times higher than that of CH_4. On the basis of adsorption isotherms, the value of IAST selectivity for CO_2/CH_4 mixtures (at the feed gas ratio of 50/50 and the pressure of 1 bar) is calculated as 60.74 (see the calculation procedures in the Supporting Information, S5). This value is among the high ranks in adsorbents and is significantly higher than that of common porous carbon. The preferential adsorption of CO_2 over CH_4 can also be attributed to the kinetically limited diffusion of CH_4 molecules, which is similar to that of N_2 molecules. The high adsorption selectivity of CO_2/CH_4 could be induced by the discrimination effects on CH_4 molecules due to the ultramicropores of the MOF-CMS. The high adoption potential of ultramicropores in the MOF-CMS can also enhance the adsorption selectivity of CO_2.

In addition to thermodynamic properties, the kinetic adsorption property also plays a crucial role in gas separation and is needed to be considered for practical applications. As shown in dynamic uptakes for O_2, N_2, CO_2, and CH_4 at different times in Figure 3c,d, these gases exhibit distinctive diffusion kinetics in the MOF-CMS. It is clearly shown that the time of reaching equilibrium is distinct from each other with different adsorbates. At the pressure increase of 1.0−1.5 bar, N_2 needs 14,800 s to reach equilibrium, while O_2 only needs 510 s to reach equilibrium. Therefore, the diffusion rate of O_2 is much faster than that of N_2. The faster diffusion rates of O_2 than N_2 can be attributed to its smaller molecular dimensions. This phenomenon is consistent with well-known CMSs in which the difference in the diffusion rates of O_2 and N_2 leads to kinetic-controlled separation for O_2/N_2. The significant difference in diffusion times between O_2 and N_2 indicates a remarkable molecular sieving effect of the MOF-CMS, which can be utilized to differentiate O_2/N_2 in air separation.[7,22] In addition to O_2/N_2, an obvious molecular sieving effect is also observed for CO_2 and CH_4. As shown in Figure 3d, CO_2 needs 800 s to reach equilibrium in the pressure increase range of 1.0−1.5 bar, while CH_4 needs 71,580 s to reach equilibrium. The time of reaching equilibrium for CO_2 is 89.7 times faster than that of CH_4. This phenomenon is in clear contrast with that of common adsorbents in which CH_4 always moves faster than CO_2.[39,40]

To evaluate the kinetic adsorption properties of O_2, N_2, CO_2, and CH_4 on the MOF-CMS quantitatively, the stretched exponential (SE) model, which is proposed by Klafter and Shlesinge, is used to simulate the kinetic adsorption profiles.[41] It has been shown that the relaxation via parallel channels and the serial hierarchically constrained dynamics can be described well using this simple model,[42,43] and its applicability to the diffusion process of gases on CMSs has also been validated by several studies.[7,18] The SE model is depicted as eq 1

$$\frac{M_t}{M_e} = 1 - e^{-(kt)^{\beta}} \tag{1}$$

where t is the time (s); M_t is the mass at time t; M_e is the mass at equilibrium; k is the stretched exponential rate constant of diffusion, which represents the intraparticle mass transfer coefficient (s^{-1}), and β is a material-dependent parameter.

As shown in Figure 3c,d, the SE model provides a good description of the experimental kinetic profiles of O_2, N_2, CO_2, and CH_4 adsorption on the MOF-CMS. Based on the SE model, the stretched exponential rate constants of diffusion at a pressure increase of 1000−2000 mbar for O_2 and N_2 are determined as 2.88×10^{-4} and 1.36×10^{-2} s^{-1}, respectively. The diffusion rate of O_2 is 47 times faster than that of N_2 under the same conditions. As for CO_2 and CH_4, the stretched exponential rate constant of diffusion with increasing pressure is 7.52×10^{-3} and 7.15×10^{-5} s^{-1} in the 1000−1500 mbar range, respectively. Compared to O_2/N_2, the difference in the diffusion rate between CO_2 and CH_4 is more significant, showing a kinetic constant ratio of 105. The great differences in diffusion rates demonstrate the outstanding molecular sieving effect for O_2/N_2 and CO_2/CH_4.

To evaluate the influence of adsorption pressure on diffusion kinetics, the diffusion rate constants for O_2, N_2, CO_2, and CH_4 at different pressures are calculated based on kinetic adsorption data (as shown in Figure 3e). It can be seen that O_2 exhibits higher diffusion rate constants than N_2 at variable pressures. The influence of pressure on diffusion rate constants for O_2 is not remarkable, but increasing pressure can impose higher diffusion rate constants for N_2. A similar phenomenon is also found in CO_2 and CH_4, except that the influence of pressure on the diffusion rates is more remarkable for CH_4 compared to that for CO_2 (as shown in Figure 3f). Thus, it can be speculated that higher pressure can accelerate the diffusion of N_2 and CH_4 in the ultramicropores of the CMS.

Compared to O_2 and CO_2, N_2 and CH_4 possess larger molecular sizes and will be more sensitive to pressure when diffusing in ultramicropores. According to Fick's Law, higher pressure means a higher driving force for diffusion, which could lead to a higher diffusion rate at a given diffusion

Table 1. Kinetic Parameters for Adsorptions of N_2, O_2, CO_2, and CH_4 on Several Porous Absorbents

name(refs)	micropore width (nm)	$D_c(N_2)$ ($m^2 \cdot s^{-1}$)	$D_c(O_2)$ ($m^2 \cdot s^{-1}$)	$D_c(CO_2)$ ($m^2 \cdot s^{-1}$)	$D_c(CH_4)$ ($m^2 \cdot s^{-1}$)
MOF-CMS (this work)	0.43[a]	1.92×10^{-13}	9.06×10^{-12}	5.01×10^{-12}	4.76×10^{-14}
CMSA[7]		4×10^{-14}	1.23×10^{-12}		
ZSM-58[44]				6.5×10^{-10}	1.03×10^{-11}
Zeolite 5A[45]				2.65×10^{-11}	
NPC-4[39]	0.52			1.8×10^{-13}	6.0×10^{-13}
NPC-7-Cu[40]	0.70	9.3×10^{-13}		5.8×10^{-13}	
$Ni_{1.5}$(4,4′-bipy)$_{1.5}$(H_3L)[46]	0.42	1.45×10^{-14}	6.41×10^{-13}	2.20×10^{-14}	
MOF-5[45,47]				1.17×10^{-9}	1.82×10^{-9}
ZIF-8[48]				5.0×10^{-10}	2.5×10^{-9}
CPM-5[49]				$7.\ 0 \times 10^{-12}$	
MOF-177[45]				2.3×10^{-9}	1.46×10^{-9}
HKUST-1[50]				1.7×10^{-9}	

[a] Calculated from the Dubinin−Radushkevich−Stoeckl (DRS) method based on CO_2 isotherm at 273.15 K.

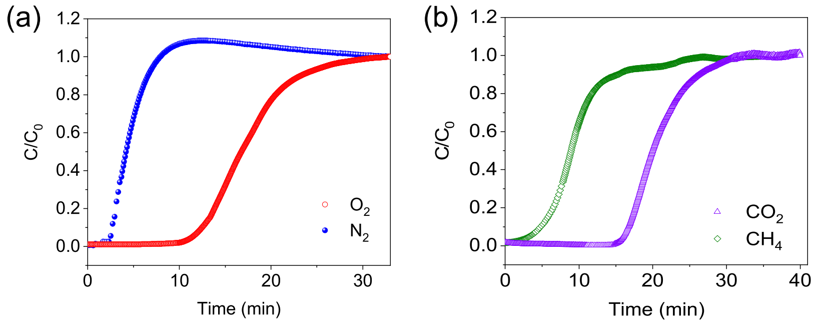

Figure 4. (a) Breakthrough plots for O_2/N_2 gas mixtures at the feed gas ratio of 0.76/0.24 at 293 K and 1 bar and (b) breakthrough plots for CO_2/CH_4 gas mixtures at the feed gas ratio of 0.95/0.05 at 293 K and 1 bar.

resistance. Based on these phenomena, we could anticipate that the pore diameter lies between the kinetic diameters of O_2/N_2 (0.346 vs 0.364 nm) and CO_2/CH_4 (0.33 vs 0.38 nm). Under the same pressure, the diffusion resistance determines how fast gas molecules diffuse in the pores. Therefore, the smaller kinetic diameters for O_2 and CO_2 give rise to their faster diffusion rates in the MOF-CMS. For gas adsorption on adsorbents with hierarchically constrained pore structures, the diffusion resistance comprises the interaction between the adsorbed gas molecules with the surface adsorption sites and the resistance induced by the small pore windows.[39] In most adsorbents, the pore windows are much larger than kinetic diameters of gas molecules, leading to rather low diffusion resistance for small gas molecules in pores. In these common adsorbents, the surface barrier is the key factor determining the diffusion behaviors for gas molecules in the pores. Therefore, N_2 and CH_4 always diffuse faster than O_2 and CO_2 due to their lower surface barriers. In the case of adsorbents with ultramicropores (like CMSs), the diffusion resistance of pore windows to gas molecules becomes the rate-determining step, while diffusion along the pore surface could be neglected. The MOF-CMS comprises pores whose diameter is near the kinetic diameters of gases; thus, the molecules with different dimensions exhibit distinct diffusion resistance along the pore windows.

Based on the stretched exponential diffusion rate constant (k), which depicts the intraparticle diffusion rate, we can calculate the overall diffusion coefficients (D_c) using the equation given below

$$k = 15D_c/r^2 \tag{2}$$

in which r is the radius of the particle.

The comparison of diffusion coefficients for the MOF-CMS with other porous absorbents (including zeolites, porous carbon, and MOF) is summarized in Table 1. As shown, the values of diffusion rate are much smaller than those of absorbents with larger pores. The ratio of $D_c(O_2)/D_c(N_2)$, which is indicative of kinetic selectivity, is 47 for O_2/N_2. This selectivity is about 8.8 times higher than that of the commercial CMSA (k_{O_2}/K_{N_2} = 5), suggesting its promising potential in air separation. In addition to O_2/N_2, the MOF-CMS also exhibits excellent kinetic selectivity for CO_2/CH_4, for which the D_c (CO_2)/D_c (CH_4) reaches 105. The much faster diffusion rates of CO_2 over CH_4 suggest that the low concentration of CO_2 in natural gas can be adsorbed preferentially on the MOF-CMS, while negligible CH_4 molecules can be adsorbed in the MOF-CMS due to its ultraslow diffusion rate along with the ultramicropores of the MOF-CMS. The combined effect can lead to the efficient capture of CO_2 from natural gas. The outstanding separation selectivity can be attributed to the existence of ultramicropores on the MOF-CMS.

Thermodynamically speaking, the MOF-CMS shows considerable adsorption selectivities for O_2/N_2 and CO_2/CH_4, while from the kinetic aspect, the O_2 and CO_2 molecules possess much faster diffusion kinetics than N_2 and CH_4. The combined effect of thermodynamic and kinetic adsorption properties suggests that the O_2 and CO_2 molecules can preferentially diffuse into the pores and are adsorbed on the pore surface by priority compared to N_2 and CH_4 molecules. Under the synergy effects of thermodynamic and kinetic properties, the O_2 and CO_2 molecules can be separated with

https://doi.org/10.1021/acsanm.2c02469
ACS Appl. Nano Mater. 2022, 5, 11414−11422

N_2 and CH_4 with much higher efficiency. Furthermore, such a thermodynamic−kinetic synergistic adsorption separation can avoid the weakness of thermodynamic and kinetic separation, such as high regeneration energy for adsorbents with highly affinitive adsorbents, the diffusion issues for adsorbents with ultramicropores, etc.

To examine the actual separation performance of the MOF-CMS, the column breakthrough experiments for O_2/N_2 and CO_2/CH_4 gas mixtures were carried out on the adsorption column packed with the MOF-CMS (see the experimental details in the Supporting Information, S2). A shown in Figure 4a, both O_2/N_2 and CO_2/CH_4 gas mixtures can be separated at the feed gas ratio of 0.76/0.24 and 0.95/0.05, which mimic the compositions of air and natural gas, respectively. Concerning O_2/N_2, N_2 elutes from the column within 2 min, whereas O_2 is retained in the column for more than 11 min. The remarkable difference in elution time between O_2 and N_2 suggests that O_2 and N_2 can be efficiently separated with the MOF-CMS. The remarkable separation performance for O_2/N_2 also shows the superiority of the MOF-CMS to common adsorbents in separating O_2/N_2, as most common adsorbents, such as active carbons and MOFs, always exhibit nearly the same breakthrough times for O_2/N_2.[51] Compared to O_2/N_2, the separation performance of CO_2/CH_4 on the MOF-CMS is more pronounced. As shown in Figure 4b, CH_4 breakthrough from the column occurs within 1 min, while CO_2 needs more than 15 min to break through the column, indicating the high selectivity toward CO_2. The clear contrast in breakthrough times for O_2/N_2 and CO_2/CH_4 suggests the outstanding separation performance of O_2/N_2 and CO_2/CH_4 on the MOF-CMS, which support the results derived from both thermodynamic and kinetic aspects. The high kinetic selectivity for O_2/N_2 and CO_2/CH_4 on the MOF-CMS can function synergistically with the high thermodynamic separation selectivity for these gases, leading to a synergistic reinforcement in separation efficiency for gas mixtures.

To further investigate the evolution process of the MOF-CMS, the carbons derived from different carbonization temperatures were prepared, and their adsorption properties were measured. The results show that carbonization temperature has a large influence on the evolution of the pore structure. At rather low carbonization temperatures (e.g., 500 °C), the as-prepared carbon shows negligible adsorption uptakes. The carbon derived at higher carbonization temperatures (e.g., 800 °C) displays a kinetic selectivity of 1.76 for CO_2/CH_4, suggesting a slight molecular sieving effect, which is similar to that common porous carbons (as shown in Figures S7 and S8 in the Supporting Information). When carbonized at 700 °C, the obtained carbon shows a clear kinetic sieving effect for CO_2/CH_4, but its kinetic selectivity is much lower than that of the MOF-CMS. It is known that the Zn(II) centers could act as the activation agent for porous carbon. Thus, it can be speculated that the activation effect of Zn(II) at higher temperatures can lead to broadening of the ultramicropores. To explore the origin of ultramicropores, the kinetic adsorption profiles of CO_2 and CH_4 on other MOF-derived carbons (including MOF-5-, ZIF-8-, and MOF-74-derived carbon) are also investigated (as shown in Figures S9−S14 in the Supporting Information). However, the carbon derived from these MOF precursors does not show any molecular sieving effect. Thus, the structural characteristics of the MOF precursor may be the main reason for the ultramicropores. The above-mentioned investigations demonstrate that the choice of the MOF precursor and proper carbonization temperature plays a vital role in forming the ultrafinepores of the MOF-CMS.

■ CONCLUSIONS

In summary, a new type of carbon molecular sieves (CMSs) was prepared from simple one-step carbonization of a metal−organic framework. Structural characterization reveals a uniform morphology and the existence of ultramicropores for this type of CMSs. Owing to its comparable pore width with the kinetic diameters of small gas molecules, it exhibits pronounced thermodynamic selectivities for O_2/N_2 and CO_2/CH_4 and significant differences in diffusion kinetics for N_2, O_2, CO_2, and CH_4. The kinetic selectivity of 47 and 105 for O_2/N_2 and CO_2/CH_4 is among the top values of selectivity of current adsorbents and outperforms that of commercial CMSs. Furthermore, the kinetic rate sequence of gas components is compatible well with their thermodynamic adsorption properties, giving rise to thermodynamic−kinetic synergistic separation. These unusual separation properties can be rationalized by the combined effects of both kinetic-controlled diffusion and overlapping adsorption potentials of ultramicropores. Breakthrough experiments validate its high separation efficiency for both O_2/N_2 and CO_2/CH_4 gas mixtures. The results reported here demonstrate that it is possible to realize a synergistic reinforcement in the separation efficiency by combining both high thermodynamic and kinetic selectivity. The outstanding performance and ease of preparation would render this type of CMSs promising potentials in applications of air separation and natural gas purification and would open a new way for preparing CMSs with novel functionalities.

■ ASSOCIATED CONTENT

Supporting Information

The Supporting Information is available free of charge at https://pubs.acs.org/doi/10.1021/acsanm.2c02469.

General information, experimental details, crystal structure of the MOF, PXRD pattern of the MOF-CMS, calculation details of the equilibrium adsorption selectivity, kinetic profiles of gas adsorption on other MOF-derived carbons, and kinetic profiles of gas adsorption on carbon carbonized at higher temperatures (PDF)

(CIF)

■ AUTHOR INFORMATION

Corresponding Authors

Liangjun Li − *Institute of New Energy, College of New Energy, China University of Petroleum (East China), Qingdao 266580, China*; Email: lilj@upc.edu.cn
Dewen Zhen − *New Energy Department, Research Institute of Petroleum Exploration & Development, China National Petroleum Corporation, Langfang 065007, China*; Email: zdw69@petrochina.com.cn
Xuebo Zhao − *Institute of New Energy, College of New Energy, China University of Petroleum (East China), Qingdao 266580, China*; orcid.org/0000-0002-5352-0953; Email: zhaoxuebo@upc.edu.cn

Authors

Dandan Liu − *Institute of New Energy, College of New Energy, China University of Petroleum (East China), Qingdao 266580, China*

Zhixing Ge − *New Energy Department, Research Institute of Petroleum Exploration & Development, China National Petroleum Corporation, Langfang 065007, China*

Xi Zhang − *New Energy Department, Research Institute of Petroleum Exploration & Development, China National Petroleum Corporation, Langfang 065007, China*

Bo Xiong − *New Energy Department, Research Institute of Petroleum Exploration & Development, China National Petroleum Corporation, Langfang 065007, China*

Zhi Li − *School of Materials Science and Engineering, Xi'an Jiaotong University, Xi'an 710054, China; New Energy Division, Shandong Energy Group Co., LTD., Zoucheng, Jining 250014, China*

Kuitong Zhang − *New Energy Division, Shandong Energy Group Co., LTD., Zoucheng, Jining 250014, China*

Tao Xing − *New Energy Division, Shandong Energy Group Co., LTD., Zoucheng, Jining 250014, China*

Wenli Xu − *Institute of New Energy, College of New Energy, China University of Petroleum (East China), Qingdao 266580, China*

Fuzhao Zhang − *Institute of New Energy, College of New Energy, China University of Petroleum (East China), Qingdao 266580, China*

Xin Gu − *Institute of New Energy, College of New Energy, China University of Petroleum (East China), Qingdao 266580, China;* orcid.org/0000-0002-6074-4146

Pengcheng Dai − *Institute of New Energy, College of New Energy, China University of Petroleum (East China), Qingdao 266580, China;* orcid.org/0000-0002-7141-8477

Complete contact information is available at:
https://pubs.acs.org/10.1021/acsanm.2c02469

Author Contributions

L.L. and D.L. contributed equally to this work. All authors have given approval to the final version of the article.

Notes

The authors declare no competing financial interest.

ACKNOWLEDGMENTS

The authors acknowledge the financial support from the Major Scientific and Technological Innovation Project of Shandong Province (2020CXGC010402), the Shandong Provincial Natural Science Foundation, China (ZR2021MB084), and the National Natural Science Foundation of China (No. 21973254). Dr. L. Li received the funding from the Major Scientific and Technological Innovation Project of Shandong Province (2020CXGC010402). Dr. L. Li and Dr. X. Gu received the funding from the Shandong Provincial Natural Science Foundation, China (ZR2021MB084). Prof. Dr. X. Zhao and Dr. L. Li received the funding from the National Natural Science Foundation of China (No. 21973254)

REFERENCES

(1) Yang, R. T. *Adsorbents: Adsorbents: Fundamentals and Applications*; John Wiley & Sons: Hoboken, 2003.

(2) Liu, C.; Zhou, Y.; Sun, Y.; Su, W.; Zhou, L. Enrichment of coal-bed methane by PSA complemented with CO_2 displacement. *AIChE J.* **2011**, *57*, 645−654.

(3) Luberti, M.; Friedrich, D.; Brandani, S.; Ahn, H. Design of a H2 PSA for cogeneration of ultrapure hydrogen and power at an advanced integrated gasification combined cycle with pre-combustion capture. *Adsorption* **2014**, *20*, 511−524.

(4) Nugent, P.; Belmabkhout, Y.; Burd, S. D.; Cairns, A. J.; Luebke, R.; Forrest, K.; Pham, T.; Ma, S.; Space, B.; Wojtas, L.; Eddaoudi, M.; Zaworotko, M. J. Porous materials with optimal adsorption thermodynamics and kinetics for CO_2 separation. *Nature* **2013**, *495*, 80−84.

(5) Kerry, F. G. *Industrial Gas Handbook: Gas Separation and Purification*; CRC Press: Boca Raton, FL, 2007.

(6) Sircar, S. Pressure swing adsorption. *Ind. Eng. Chem. Res.* **2002**, *41*, 1389−1392.

(7) Chagger, H. K.; Ndaji, F. E.; Sykes, M. L.; Thomas, K. M. Kinetics of adsorption and diffusional characteristics of carbon molecular sieves. *Carbon* **1995**, *33*, 1405−1411.

(8) Hassan, M. M.; Ruthven, D. M.; Raghavan, N. S. Air separation by pressure swing adsorption on a carbon molecular sieve. *Chem. Eng. Sci.* **1986**, *41*, 1333−1343.

(9) Taylor, M. K.; Runcevski, T.; Oktawiec, J.; Bachman, J. E.; Siegelman, R. L.; Jiang, H.; Mason, J. A.; Tarver, J. D.; Long, J. R. Near-Perfect CO_2/CH_4 Selectivity Achieved through Reversible Guest Templating in the Flexible Metal−Organic Framework Co(bdp). *J. Am. Chem. Soc.* **2018**, *140*, 10324−10331.

(10) Xu, H.; He, Y.; Zhang, Z.; Xiang, S.; Cai, J.; Cui, Y.; Yang, Y.; Qian, G.; Chen, B. A microporous metal−organic framework with both open metal and Lewis basic pyridyl sites for highly selective C_2H_2/CH_4 and C_2H_2/CO_2 gas separation at room temperature. *J. Mater. Chem. A* **2013**, *1*, 77−81.

(11) Chen, K.-J.; Madden, D. G.; Pham, T.; Forrest, K. A.; Kumar, A.; Yang, Q.-Y.; Xue, W.; Space, B.; Perry, J. J.; Zhang, J.-P.; Chen, X.-M.; Zaworotko, M. J. Tuning Pore Size in Square-Lattice Coordination Networks for Size-Selective Sieving of CO_2. *Angew. Chem., Int. Ed.* **2016**, *55*, 10268−10272.

(12) Lv, X.; Li, L.; Tang, S.; Wang, C.; Zhao, X. High CO_2/N_2 and CO_2/CH_4 selectivity in a chiral metal-organic framework with contracted pores and multiple functionalities. *Chem. Commun.* **2014**, *50*, 6886−6889.

(13) Yang, Q.; Wiersum, A. D.; Jobic, H.; Guillerm, V.; Serre, C.; Llewellyn, P. L.; Maurin, G. Understanding the Thermodynamic and Kinetic Behavior of the CO_2/CH_4 Gas Mixture within the Porous Zirconium Terephthalate UiO-66(Zr): A Joint Experimental and Modeling Approach. *J. Phys. Chem. C* **2011**, *115*, 13768−13774.

(14) Peng, Y.-L.; Wang, T.; Jin, C.; Deng, C.-H.; Zhao, Y.; Liu, W.; Forrest, K. A.; Krishna, R.; Chen, Y.; Pham, T.; Space, B.; Cheng, P.; Zaworotko, M. J.; Zhang, Z. Efficient propyne/propadiene separation by microporous crystalline physiadsorbents. *Nat. Commun.* **2021**, *12*, No. 5768.

(15) Wu, X.-Q.; Xie, Y.; Liu, J.-H.; He, T.; Zhang, Y.-Z.; Yu, J.; Kong, X.-J.; Li, J.-R. Integrating multiple adsorption sites and tortuous diffusion paths into a metal−organic framework for C_3H_4/C_3H_6 separation. *J. Mater. Chem. A* **2019**, *7*, 25254−25257.

(16) Kapoor, A.; Yang, R. T. Kinetic separation of methane—carbon dioxide mixture by adsorption on molecular sieve carbon. *Chem. Eng. Sci.* **1989**, *44*, 1723−1733.

(17) Cui, W.-G.; Hu, T.-L.; Bu, X.-H. Metal−Organic Framework Materials for the Separation and Purification of Light Hydrocarbons. *Adv. Mater.* **2020**, *32*, No. 1806445.

(18) Xing, Y.; Cai, J.; Li, L.; Yang, M.; Zhao, X. An exceptional kinetic quantum sieving separation effect of hydrogen isotopes on commercially available carbon molecular sieves. *Phys. Chem. Chem. Phys.* **2014**, *16*, 15800−15805.

(19) Bae, Y. S.; Lee, C. H. Sorption kinetics of eight gases on a carbon molecular sieve at elevated pressure. *Carbon* **2005**, *43*, 95−107.

(20) Mohamed, A. R.; Mohammadi, M.; Darzi, G. N. Preparation of carbon molecular sieve from lignocellulosic biomass: A review. *Renew. Sust. Energ. Rev.* **2010**, *14*, 1591−1599.

(21) Moore, S. V.; Trimm, D. L. The preparation of carbon molecular sieves by pore blocking. *Carbon* **1977**, *15*, 177−180.

(22) Reid, C. R.; Thomas, K. M. Adsorption of Gases on a Carbon Molecular Sieve Used for Air Separation: Linear Adsorptives as Probes for Kinetic Selectivity. *Langmuir* **1999**, *15*, 3206−3218.

(23) Furukawa, H.; Cordova, K. E.; O'Keeffe, M.; Yaghi, O. M. The Chemistry and Applications of Metal-Organic Frameworks. *Science* **2013**, *341*, 1230444.

(24) Cadiau, A.; Belmabkhout, Y.; Adil, K.; Bhatt, P. M.; Pillai, R. S.; Shkurenko, A.; Martineau-Corcos, C.; Maurin, G.; Eddaoudi, M. Hydrolytically stable fluorinated metal-organic frameworks for energy-efficient dehydration. *Science* **2017**, *356*, 731−735.

(25) Yang, S. J.; Kim, T.; Im, J. H.; Kim, Y. S.; Lee, K.; Jung, H.; Park, C. R. MOF-Derived Hierarchically Porous Carbon with Exceptional Porosity and Hydrogen Storage Capacity. *Chem. Mater.* **2012**, *24*, 464−470.

(26) Li, L.; Wang, Y.; Gu, X.; Yang, Q.; Zhao, X. Increasing the CO_2/N_2 Selectivity with a Higher Surface Density of Pyridinic Lewis Basic Sites in Porous Carbon Derived from a Pyridyl-Ligand-Based Metal−Organic Framework. *Chem. Asian J.* **2016**, *11*, 1913−1920.

(27) Xu, Y.; Tu, W.; Zhang, B.; Yin, S.; Huang, Y.; Kraft, M.; Xu, R. Nickel Nanoparticles Encapsulated in Few-Layer Nitrogen-Doped Graphene Derived from Metal−Organic Frameworks as Efficient Bifunctional Electrocatalysts for Overall Water Splitting. *Adv. Mater.* **2017**, *29*, No. 1605957.

(28) Xia, W.; Mahmood, A.; Zou, R.; Xu, Q. Metal-organic frameworks and their derived nanostructures for electrochemical energy storage and conversion. *Energy Environ. Sci.* **2015**, *8*, 1837−1866.

(29) Li, L.; Tang, S.; Lv, X.; Jiang, M.; Wang, C.; Zhao, X. An rht type metal-organic framework based on small cubicuboctahedron supermolecular building blocks and its gas adsorption properties. *New J. Chem.* **2013**, *37*, 3662−3670.

(30) Nouar, F.; Eubank, J. F.; Bousquet, T.; Wojtas, L.; Zaworotko, M. J.; Eddaoudi, M. Supermolecular Building Blocks (SBBs) for the Design and Synthesis of Highly Porous Metal-Organic Frameworks. *J. Am. Chem. Soc.* **2008**, *130*, 1833−1835.

(31) Pinto, M. L.; Mestre, A. S.; Carvalho, A. P.; Pires, Jo. Comparison of Methods to Obtain Micropore Size Distributions of Carbonaceous Materials from CO_2 Adsorption Based on the Dubinin−Radushkevich Isotherm. *Ind. Eng. Chem. Res.* **2010**, *49*, 4726−4730.

(32) Cazorla-Amorós, D.; Alcañiz-Monge, J.; Linares-Solano, A. Characterization of Activated Carbon Fibers by CO_2 Adsorption. *Langmuir* **1996**, *12*, 2820−2824.

(33) Cazorla-Amorós, D.; Alcañiz-Monge, J.; de la Casa-Lillo, M. A.; Linares-Solano, A. CO_2 As an Adsorptive To Characterize Carbon Molecular Sieves and Activated Carbons. *Langmuir* **1998**, *14*, 4589−4596.

(34) Li, P.; Handan Tezel, F. Adsorption separation of N_2, O_2, CO_2 and CH_4 gases by β-zeolite. *Microporous Mesoporous Mater.* **2007**, *98*, 94−101.

(35) Min, J. G.; Kemp, K. C.; Kencana, K. S.; Hong, S. B. Silver-exchanged CHA zeolite as a CO_2-resistant adsorbent for N_2/O_2 separation. *Microporous Mesoporous Mater.* **2021**, *323*, No. 111239.

(36) Nabais, J. M. V.; Carrott, P. J. M.; Carrott, M. M. L. R.; Padre-Eterno, A. M.; Menéndez, J. A.; Dominguez, A.; Ortiz, A. L. New acrylic monolithic carbon molecular sieves for O_2/N_2 and CO_2/CH_4 separations. *Carbon* **2006**, *44*, 1158−1165.

(37) Myers, A. L.; Prausnitz, J. M. Thermodynamics of mixed-gas adsorption. *AIChE J.* **1965**, *11*, 121−127.

(38) Fu, Y.; Liu, Y.; Li, Z.; Zhang, Q.; Yang, X.; Zhao, C.; Zhang, C.; Wang, H.; Yang, R. T. Insights into adsorption separation of N2/O2 mixture on FAU zeolites under plateau special conditions: A molecular simulation study. *Sep. Purif. Technol.* **2020**, *251*, No. 117405.

(39) Li, L.; Bell, J. G.; Tang, S.; Lv, X.; Wang, C.; Xing, Y.; Zhao, X.; Thomas, K. M. Gas Storage and Diffusion through Nanocages and Windows in Porous Metal−Organic Framework Cu_2(2,3,5,6-tetramethylbenzene-1,4-diisophthalate)$(H_2O)_2$. *Chem. Mater.* **2014**, *26*, 4679−4695.

(40) Li, L.; Xue, H.; Wang, Y.; Zhao, P.; Zhu, D.; Jiang, M.; Zhao, X. Solvothermal Metal Metathesis on a Metal−Organic Framework with Constricted Pores and the Study of Gas Separation. *ACS Appl. Mater. Interfaces* **2015**, *7*, 25402−25412.

(41) Klafter, J.; Shlesinger, M. F. On the relationship among three theories of relaxation in disordered systems. *Proc. Natl. Acad. Sci. U.S.A.* **1986**, *83*, 848−851.

(42) Zhao, X.; Xiao, B.; Fletcher, A. J.; Thomas, K. M.; Bradshaw, D.; Rosseinsky, M. J. Hysteretic Adsorption and Desorption of Hydrogen by Nanoporous Metal-Organic Frameworks. *Science* **2004**, *306*, 1012−1015.

(43) Wang, C.; Li, L.; Bell, J. G.; Lv, X.; Tang, S.; Zhao, X.; Thomas, K. M. Hysteretic Gas and Vapor Sorption in Flexible Interpenetrated Lanthanide-Based Metal−Organic Frameworks with Coordinated Molecular Gating via Reversible Single-Crystal-to-Single-Crystal Transformation for Enhanced Selectivity. *Chem. Mater.* **2015**, *27*, 1502−1516.

(44) Bleken, B.-T. L.; Lillerud, K. P.; Splith, T.; Pusch, A.-K.; Stallmach, F. PFG NMR diffusion measurements of CH_4 and CO_2 through large ZSM-58-crystals. *Microporous Mesoporous Mater.* **2013**, *182*, 25−31.

(45) Saha, D.; Bao, Z.; Jia, F.; Deng, S. Adsorption of CO_2, CH_4, N_2O, and N_2 on MOF-5, MOF-177, and Zeolite 5A. *Environ. Sci. Technol.* **2010**, *44*, 1820−1826.

(46) Zhao, X.; Bell, J. G.; Tang, S.-F.; Li, L.; Thomas, K. M. Kinetic molecular sieving, thermodynamic and structural aspects of gas/vapor sorption on metal organic framework $[Ni_{1.5}$(4,4[prime or minute]-bipyridine)$_{1.5}(H_3L)(H_2O)_3][H_2O]_7$ where H_6L = 2,4,6-trimethylbenzene-1,3,5-triyl tris(methylene)triphosphonic acid. *J. Mater. Chem. A* **2016**, *4*, 1353−1365.

(47) Zhao, Z.; Li, Z.; Lin, Y. S. Adsorption and Diffusion of Carbon Dioxide on Metal−Organic Framework (MOF-5). *Ind. Eng. Chem. Res.* **2009**, *48*, 10015−10020.

(48) Bux, H.; Chmelik, C.; van Baten, J. M.; Krishna, R.; Caro, J. Novel MOF-Membrane for Molecular Sieving Predicted by IR-Diffusion Studies and Molecular Modeling. *Adv. Mater.* **2010**, *22*, 4741−4743.

(49) Sabouni, R.; Kazemian, H.; Rohani, S. Mathematical Modeling and Experimental Breakthrough Curves of Carbon Dioxide Adsorption on Metal Organic Framework CPM-5. *Environ. Sci. Technol.* **2013**, *47*, 9372−9380.

(50) Tovar, T. M.; Zhao, J.; Nunn, W. T.; Barton, H. F.; Peterson, G. W.; Parsons, G. N.; LeVan, M. D. Diffusion of CO_2 in Large Crystals of Cu-BTC MOF. *J. Am. Chem. Soc.* **2016**, *138*, 11449−11452.

(51) Thallapally, P. K.; Banerjee, D.; Elsaidi, S. Xe Adsorption and Separation Properties of a Series of Mi-croporous Metal-Organic Frameworks (MOFs) with V-shaped Link-ers. *J. Mater. Chem. A* **2017**, *5*, 16611−16615.